Twelfth International
WORKSHOP ON WATER WAVES AND FLOATING BODIES

VISCOUS EFFECTS IN WAVE–BODY INTERACTION

M. Landrini †, M. Ranucci §, C.M. Casciola §, G. Graziani §
† INSEAN, Via di Vallerano 139, 00128 Roma (Italy)
§ Dipartimento di Meccanica e Aeronautica, Università di Roma *La Sapienza*

1 Introduction

The flow of an incompressible viscous fluid about a circular cylinder beneath a regular Stokes wave train is a typical problem in marine structures hydrodynamics and several theoretical and experimental results are available.

The accurate experimental analysis by Chaplin [5] confirms that the vertical mean value of the hydrodynamic force as well as the second and third harmonics of the fluctuating components are well explained in terms of the inviscid diffraction of the incident wave field as is described by weakly nonlinear models [7, 8], and by fully nonlinear computations [6]. However, the potential theory fails to capture exhaustively the entire phenomenon. Actually, Chaplin's results revealed a significant reduction in the amplitude of the fundamental harmonic of the loading which cannot be related to the purely inviscid diffraction of the incoming waves.

For a cylinder with small submergence, the nonlinear dynamics of the wave system is crucial and tightly coupled to the dynamics of the vorticity field about the body. In these conditions, we have to consider the full Navier–Stokes equations for a free surface flow. To this purpouse, a particle method which account for viscous effects and flow separation near the body is deviced and the nonlinear behaviour of the free surface is fully considered (see also Yeung [9] for a similar approach in the context of roll motion of ship cross–sections).

2 Description of the mathematical problem

We consider a circular cylinder $\mathcal{B}$ immersed beneath a regular wave train on the free surface $\mathcal{F}$. The water depth is assumed infinite and the fluid domain $\mathcal{D}$ is unbounded in the horizontal direction. The motion of the viscous incompressible fluid within $\mathcal{D}$ is described by the Navier–Stokes equations. The standard no–slip condition must be satisfied on the solid boundary $\partial\mathcal{B}$ and the kinematic and dynamic conditions hold at the free surface. Actually, we neglect the effects of the free surface boundary layer and assume the support of the body–generated vorticity to be confined away from the free interface. Consistently the dynamic boundary condition on $\mathcal{F}$ simply requires the fluid pressure to be atmospheric. Under such hypothesis, for finite times and far from the body, the fluid motion reduces to an irrotational wave system. In particular, we consider the corresponding Stokes wave field as a basis flow and solve for the correction which describes both viscous and diffraction effects.

In order to analyze the vortical flow around the body and its interaction with the free surface, a vorticity–velocity formulation is considered, and an operator splitting approach is adopted for the numerical solution. The algorithm approximates the flow evolution by a sequence of diffusive and convective steps according to the Stokes and Euler equations, respectively. In particular, the diffusion of the vorticity is described through the solution of the heat transfer equation, the advection step consists in evaluating the Lagrangian motion of the vortical particles, while the free surface evolves according to a purely inviscid dynamics. To enforce the no–slip boundary condition, following Chorin [1], a vortex sheet is inserted on the body contour after each convective step. This vortex sheet is furtherly lumped in order to obtain the circulation of the discrete vortices which are diffused together with those already existing within the flow field. The solution of the problem is effectively achieved by means of a fast vortex method coupled to an integral representation of the velocity field.

In order to describe the diffusion of the vorticity, a deterministic approach based on the integral representation for the diffusion problem is adopted as discussed in [2] for flows without a free surface. Consistently with this particle scheme, the evolution of the free surface is described through the motion of markers distributed on $\mathcal{F}$ by using kinematic and dynamic evolution equations expressed in terms of velocity components [4].

Finally, the perturbation velocity field in the fluid domain is expressed in terms of the Poincaré representation formula [3]. At each convective–step, a boundary integral equation is first solved to determine the normal velocity

component on $\mathcal{F}$ and the tangential velocity component on $\partial\mathcal{B}$ and then the velocity field in $\mathcal{D}$ is explicitely computed through the integral representation.

3 Computational results

The above described algorithm is used to analyze the interaction of a Stokes wave train with a submerged circular cylinder in order to enlight the role of the viscosity. The solutions of the Navier–Stokes equations are compared with those provided by an inviscid model which usually fully captures the nonlinear dynamics of wave–body interactions as well as with the experiments reported in [5]. In particular, Chaplin's Case–E ($kR = 0.206$, $h/R = 2.0$) is considered in detail since non–linear diffraction effects are expected to be more pronounced for shallow submergences of the cylinder.

By examining the wave patterns reported in figure 1 for $t/T_S = 10$ and $K_c = 0.75$, a first comparison between the viscous (black line) and inviscid (red line) solutions is possible. Qualitatively, the wave diffraction dynamics appears to be unaltered by the vorticity generated at the body boundary: however, although the two solutions appear to be coincident for low values of K_c, an increasingly pronounced difference can be detected for larger values, the amplitude of the emitted shorter wavelenghts appearing to be reduced in the viscous solution. Consistently, the wave induced loading predicted by the viscous and by the inviscid model coincides for the smaller K_c and show significant discrepancies for the largest value. In particular, the time evolution of the two force components F_x, F_y is reported in figure 2 for $K_c = 1.0$. In this figure, after an initial transient of about one wave period during which the viscous (black lines) and the inviscid solutions (red lines) are substantially superimposed, the viscous loads oscillate with different amplitudes with respect to the inviscid ones. In both cases the time behavior of the force displays an apparent non–sinusoidal shape which manifests the non–linear effects in the wave–body interaction.

Since the detected differencies between the two solutions are related to the generation and to the following evolution of the vorticity, it is worthwhile to discuss the dynamics of the rotational field. A typical vorticity distribution is shown in figure 3 where cyan–blue region denote the positive values (*i.e.* clockwise) and red–yellow region the negative ones. Two intense vorticity layers of opposite sign which are driven by the rotating flow induced by the waves may be observed. Then, due to the diffusion, the vorticity is furtherly spread away from the cylinder, a thickened structure is generated and new vortex layers, of opposite sign, possibly appear on the body. Finally, the interaction of opposite signed layers takes place, originating the well defined structure observed in the figure above the cylinder. Near the body the vorticity field becomes periodic soon after the beginning of the flow evolution while the *far* field dynamics does not significantly affect the forces acting on the body.

A quantitative assessment of this behaviour can be gained through the analysis of the mean value over a period of the circulation along circles concentric with the cylinder, figure 4. In particular the black, red and green lines refer to $t/T_s = 18$, 19 and 20, respectively. A steady mean circulation is estabilished about the cylinder while farther from the body the dynamics of the far field vorticity still maintains a considerable time dependance. In his analysis of the nonlinear behaviour of wave induced loads, Chaplin pointed out the mean circulation about the cylinder as the key feature to explain the marked decreasing of the actual inertia coefficient with respect to the potential flow prediction. This difference emerges from figure 5, where the present inviscid solution (black line) always exceeds Chaplin's experimental data. The correct behaviour is fully recovered by the viscous solution shown in the same plot (red symbols), thus confirming the relevance of the diffusion for this force components.

References

[1] Chorin A. J. (1973): Numerical study of slightly viscous flow. *J. Fluid Mech.*, **57**, 785-796.

[2] Graziani G., Ranucci M., Piva R. (1995): From a Boundary Integral Formulation to a Vortex Method for Viscous Flows, *Comput. Mech.*, **15**, 4, 301-314.

[3] Bassanini, P., Casciola, C. M., Lancia, M. R. & Piva R. 1991 A boundary integral formulation for the kinetic field in aerodynamics. Part I. *Europ. J. Mech.*, B/Fluids, **10**(6), 605-627.

[4] Casciola, C. M. & Landrini, M. 1996 Nonlinear long waves generated by a moving pressure disturbance *J. Fluid Mech.*, **325** 399–418.

[5] Chaplin., J.R. 1984 Nonlinear forces on a horizontal cylinder beneath waves. *Journal of Fluid Mechanics*, **147**,pp 449–464.

[6] Y. Liu, D.G. Dommermuth, D.K.P. Yue. A high–order spectral method for nonlinear wave–body interactions. *Journal of Fluid Mechanics*, 245:115–136, 1992.

[7] T. F. OGILVIE. First and second order forces on a circular cylinder submerged under a free surface. *Journal of Fluid Mechanics*, 16:451–472, 1963.

[8] T. VADA. A numerical solution of the second–order wave–diffraction problem for a submerged cylinder of arbitrary shape. *Journal of Fluid Mechanics*, 174:23–37, 1987.

[9] R. W. YEUNG, C. CERMELLI, S. W. LIAO Vorticity fields due to rolling bodies in a free surface – Experiment and Theory. 21^{st} Symposium on Naval Hydrodynamics, Trondheim, Norway, 1996.

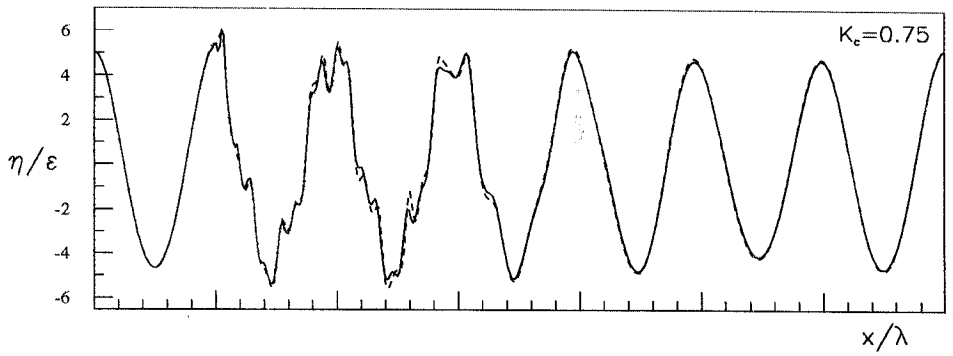

Figure 1: Free surface profiles for $K_c = 0.75$ and $t/T_S = 10$. Comparison of viscous (solid line) and inviscid (dashed line) solutions.

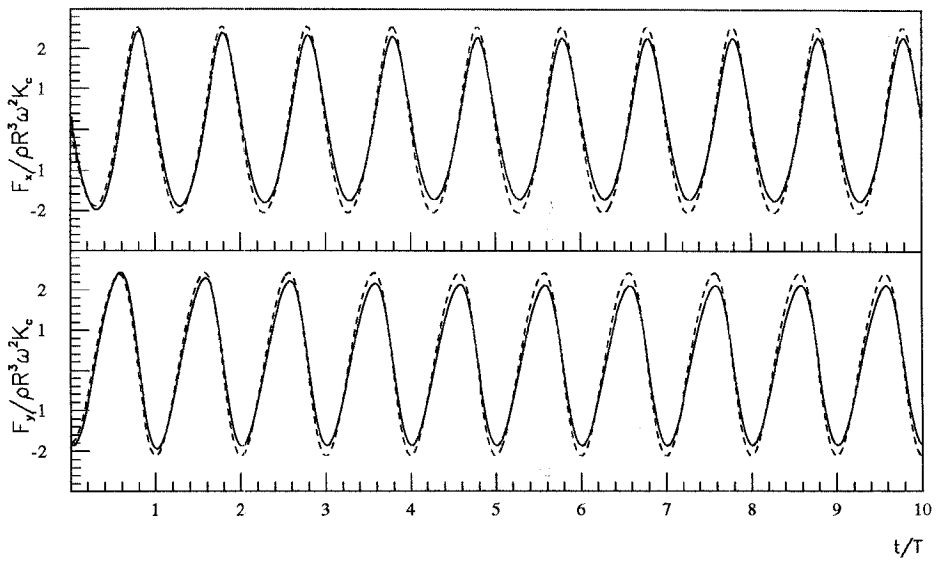

Figure 2: Evolution in time of horizontal (upper plot) and vertical (lower plot) force components ($K_c = 0.75$). Comparison of the viscous (solid lines) and inviscid (dashed lines) solutions.

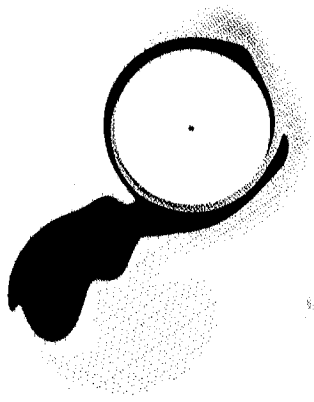

Figure 3: Vorticity field around the circular cylinder at $t/Ts = 10$, $K_c = 0.75$.

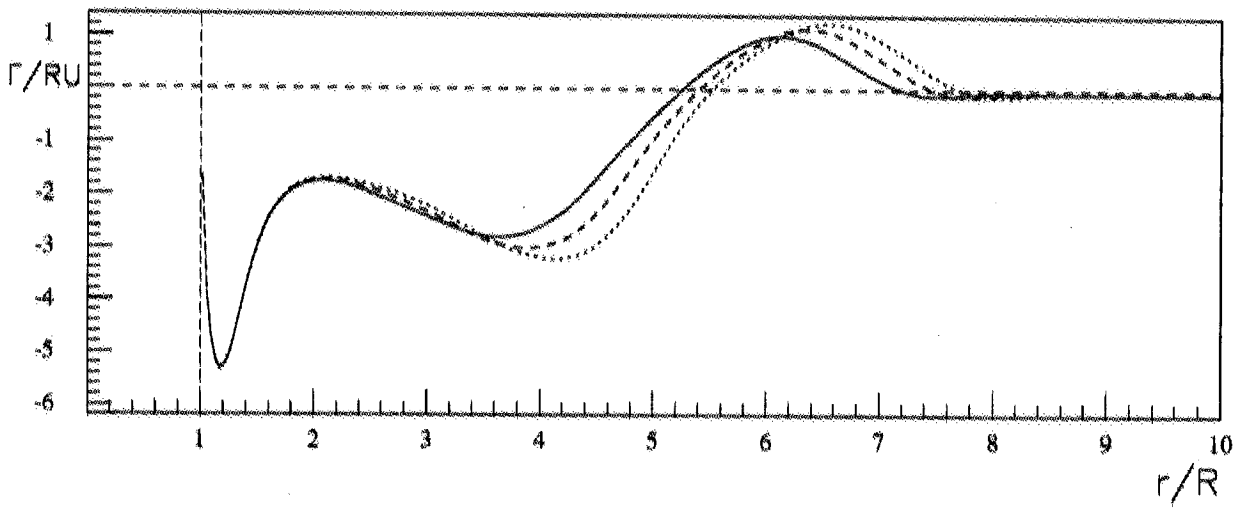

Figure 4: Total mean circulation about circles of increasing radius r ($K_c = 0.75$). The three curves refer to $t/Ts = 18, 19, 20$ (solid, dashed and dotted lines respectively).

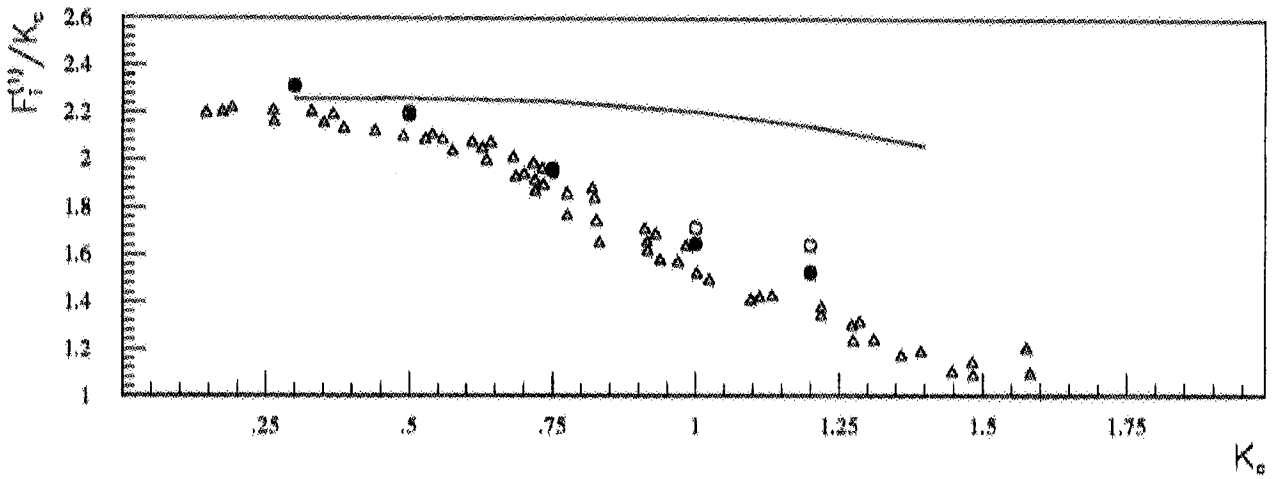

Figure 5: Fundamental spectral component of horizontal and vertical forces on the cylinder. (triangles: Chaplin's data, circles: present viscous solution, solid line: present inviscid solution)